Targeted Search for Effective Intermediate Band Solar Cell Materials

Joseph T. Sullivan, Christie B. Simmons, Tonio Buonassisi, and Jacob J. Krich

***Abstract*—Recent years have seen a number of candidate materials for intermediate band (IB) solar cells, but none has demonstrated a high-efficiency device. We explain this deficit by means of a figure of merit, which predicts the potential effectiveness of candidate IB materials in advance of device fabrication. This figure of merit captures in a single parameter the inherent tradeoff between enhanced absorption and enhanced recombination within an IB material, and it suggests a path toward efficient IB materials. We illustrate a screening approach based on this figure of merit for a specific class of IB material systems: a dopant-induced impurity band in silicon. We show, in this case, that the optical and nonradiative electrical trapping cross sections of impurities, widely studied properties that can be measured in bulk materials, determine the potential performance of IB solar cell devices. We conclude with a list of appealing and unappealing candidate material systems.**

***Index Terms*—Charge carrier lifetime, impurity photovoltaic, intermediate band photovoltaic, mathematical model, photovoltaic cells.**

I. Introduction

The intermediate band solar cell (IBSC) [1] has the possibility to break the Shockley–Queisser efficiency limit [2] for standard pn-junction solar cells. The high efficiency relies on an intermediate band (IB) material—a semiconductor with an extra set of partially filled levels contained entirely inside the bandgap, as illustrated in Fig. 1. This IB material allows absorption of two subgap photons to move an electron from valence band (VB) to conduction band (CB), while the voltage can be set by the larger bandgap. For high efficiency, the bandgaps of the IBSC must be well matched to the solar spectrum, and there must be more carriers gained from optical absorption than lost to recombination in the IB material.

There are no known naturally occurring IB materials, but many IB materials have been produced artificially, using quantum dots or quantum wells, highly mismatched alloys, or deep-level dopants, as reviewed in [3]. A number of these have demonstrated the two-photon-induced photocurrent that is the hallmark of IBSC activity [4]–[7], but overall power conversion efficiencies have remained low [7]–[9]. These low efficiencies are likely due in large part to fast nonradiative recombination, which is made worse by mid-level states in the gap [10]. Producing high-efficiency IBSC's also requires optimized cell architectures with high-quality contacts and junctions; therefore, low efficiency in a laboratory device does not necessarily indicate a failure of the IBSC mechanism.

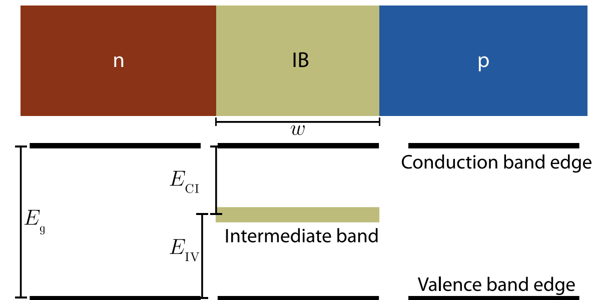

Fig. 1. Schematic of IBSC and idealized energy level diagram with the standard n-IB-p structure, with an IB of width w. Sunlight is incident from the left. The energy gaps E_g, E_{IV}, and E_{CI} must be well matched to the solar spectrum to achieve high efficiency [1].

To assess the potential efficiency of candidate IB materials, we want a figure of merit independent of the other cell components and interfaces. A good figure of merit is easily measured and has good predictive ability as to whether it would be worthwhile to construct a full device. So far, the most commonly used figures of merit are the bandgaps of the IB—they must be well matched to the solar spectrum, with current matching between the two subgap transitions; the ideal bandgap under full concentration is 1.9 eV with an IB 0.7 eV away from one of the band edges [1]. Bandgaps alone, however, cannot predict performance of a realistic IB material with nonradiative recombination. Krich *et al.* [11] proposed a figure of merit ν that captures the balance between the absorption and recombination processes in the IB material. It depends only on the material's bandgap, subgap absorptivity, mobility, and lifetime. Measurement of ν have been performed on a candidate IB material, silicon hyperdoped with high concentrations of sulfur [12], [13], concluding that lower concentrations of sulfur would be advantageous.

In this manuscript, we show that the figure of merit ν can also be used to predict which materials have the potential to make effective IBSC's before any growth or fabrication, allowing targeted search for effective IB materials. This effort is similar in spirit to that in [14], but including effects of nonradiative processes. Our goal is to present a simple theory amenable to screening candidate IB materials without detailed modeling of each one. We describe the figure of merit ν and its

Manuscript received June 24, 2014; revised October 5, 2014; accepted October 8, 2014. Date of publication November 5, 2014; date of current version December 18, 2014. The work at the Massachusetts Institute of Technology was supported by the National Science Foundation grant for Energy, Power, and Adaptive Systems under Contract ECCS-1102050. The work in Ottawa was supported by the Natural Sciences and Engineering Research Council of Canada (NSERC) and the NSERC Photovoltaic Innovation Network.

J. T. Sullivan, C. B. Simmons, and T. Buonassisi are with the Massachusetts Institute of Technology, Cambridge, MA 02139 USA (e-mail: jts48@cornell.edu; simmonsc@mit.edu; buonassisi@mit.edu).

J. J. Krich is with the Department of Physics, University of Ottawa, Ottawa, ON K1N 6N5, Canada (e-mail: jkrich@uottawa.ca).

Color versions of one or more of the figures in this paper are available online at http://ieeexplore.ieee.org.

Digital Object Identifier 10.1109/JPHOTOV.2014.2363560

2156-3381 © 2014 IEEE. Personal use is permitted, but republication/redistribution requires IEEE permission.
See http://www.ieee.org/publications_standards/publications/rights/index.html for more information.

implications in new detail (see Section II) and demonstrate the prediction of ν for various deep-level dopants in silicon (see Section III).

II. Figure of Merit

As first outlined in [11], we can construct a figure of merit by considering an IBSC where the IB region is the optimal thickness to balance the extra subgap absorption and nonradiative recombination. Without any detailed modeling, we expect an effective IBSC to have an IB region thick enough to produce an optical depth for subgap light, OD, of order 1, ensuring the material can absorb sufficient subgap light to be useful; we confirm this statement below with more detailed modeling. We approximate OD by taking the average subgap absorptivity α and consider that the IB region has width $w = \alpha^{-1}$; therefore, OD$\equiv \alpha w = 1$. Note that OD describes reductions of light intensity by powers of e.

To be efficient, such a device should have $\tau/t \gg 1$, where τ is the carrier (electron or hole) lifetime, and t is the time to traverse the IB region. We consider two cases. First, if the built-in potential $V_{\rm bi}$ drops smoothly across the IB region (as in a p-i-n structure or, e.g., a quantum-dot-based IB), then the transit time in the electric field $E = V_{\rm bi}/w$ is

$$t_{\rm drift} = \frac{w}{\mu E} = \frac{w^2}{\mu V_{\rm bi}} = (\mu V_{\rm bi}\alpha^2)^{-1} \quad (1)$$

where μ is the carrier mobility. We then find $\tau/t = V_{\rm bi}\mu\alpha^2\tau$. Since $V_{\rm bi} \leq E_{\rm g}/q$, where $E_{\rm g}$ is the bandgap and q is the electric charge, we can replace $V_{\rm bi}$ by $E_{\rm g}/q$ to make the figure of merit[1]

$$\nu_{\rm drift} = \frac{E_{\rm g}}{q}\mu\alpha^2\tau. \quad (2)$$

Second, if the IB material forms junctions with the surrounding n- and p-type regions that are thin compared with w, then there is no electric field in the majority of the IB region, and the carriers must diffuse with diffusion constant D. In this case, the traversal time is

$$t_{\rm diff} = \frac{w^2}{D} = \frac{q}{k_{\rm b}T\mu\alpha^2} \quad (3)$$

where $k_{\rm b}$ is the Boltzmann constant, T is the temperature, and we have used the Einstein relation to connect D to μ. In this case, we find a figure of merit for the diffusive case

$$\nu_{\rm diff} = \frac{k_{\rm b}T}{q}\mu\alpha^2\tau \quad (4)$$

which is the same as (2) except with the energy scale $E_{\rm g}$ reduced to $k_{\rm b}T$, reflecting the smaller driving force for diffusion. Equation (4) first appeared in [15]. Note that light trapping in the IB region could maintain OD of order 1 while decreasing w to $w_{\rm trap} < \alpha^{-1}$. With such light trapping, the figures of merit would increase by the factor $(w_{\rm trap}\alpha)^{-2}$; light trapping by random texturing [16] can make this factor $(4n_s^2)^2$, where n_s is the index of refraction, which gives a trapping enhancement of approximately 2000 in silicon.

[1] Note that [11] had $V_{\rm bi}$ in place of $E_{\rm g}/q$. Since $E_{\rm g}$ is a material property of the IB region alone, it is preferable to replace $V_{\rm bi}$ by $E_{\rm g}/q$.

These figures of merit depend only on properties of the IB material itself and, thus, can be measured without making full solar cell devices. In an effective IB device, ν should be large for both electrons and holes; therefore, the mobility, lifetime, and absorptivity need to be determined for both carrier types. Interface recombination at edges of the IB region could impact the effective lifetime of carriers in the IB, but for the model here, τ represents the bulk carrier lifetime in the IB material.

Selecting the appropriate figure of merit ($\nu_{\rm diff}$ or $\nu_{\rm drift}$) to estimate an IB material's performance requires knowledge of the absorption coefficient and an estimate of the depletion width within the IB; generally speaking, highly absorbing materials could have a thinner and potentially fully depleted IB layer, while a weakly absorbing IB material would require a thicker layer and would, therefore, likely be diffusion limited.

Large ν is a necessary but not sufficient condition for an efficient IBSC. In addition to having large ν for both electrons and holes, an efficient IBSC must have bandgaps well matched to the solar spectrum, as well as the usual requirements for the remainder of the device, including high-quality p- and n-type regions with low-resistance and low-recombination interfaces and antireflection coatings. The figure of merit ν is most informative for devices with nonradiative lifetimes dominating radiative lifetimes, as in all current candidate materials; for ultrahigh efficiency IBSC, approaching the thermodynamic limits [1], a modified external luminescent efficiency will be the most effective figure of merit [17].

Device models permit the determination of how large ν must be for an IBSC to produce an increase in device efficiency. We show the qualitative results by considering a model for an IBSC in the diffusive limit, described in [15], with full details to be given in a future work. The key feature is that we must have $\nu \gtrapprox 1$ to achieve significant improvements from an IBSC. The model includes minority carrier diffusion equations, the depletion approximation near the junctions, law-of-the-junction boundary conditions [18] modified for an n-IB-p structure [15], and no photon recycling. We have chosen ideal n and p regions, in order to focus on the effects of IB quality, and ν is the same for electrons and holes. The top n-type layer is thick enough to absorb all incoming photons with energy greater than E_g. The thickness of the IB region, giving the subgap optical depth OD, has been chosen to be optimal at each value of ν.

Fig. 2 shows efficiency as a function of ν within this model for two example IBSC's. One has the ideal bandgaps for full concentration, $E_g = 1.9$ eV and $E_{\rm CI} = 0.7$ eV [1], while the other is modeled on silicon, with $E_g = 1.1$ eV and $E_{\rm CI} = 0.35$ eV. Both have nonoverlapping absorptions, IB filling factor $f = 1/2$, and electron and hole optical and trapping cross sections and mobilities set to be equal. In both cases, for ν considerably less than 1, the optimal IBSC has no IB at all (w, OD$\rightarrow 0$), and the efficiency is essentially that of the np-junction solar cell alone. For large ν, the material can become radiatively limited, requiring a model with photon recycling to capture the true efficiency limit.

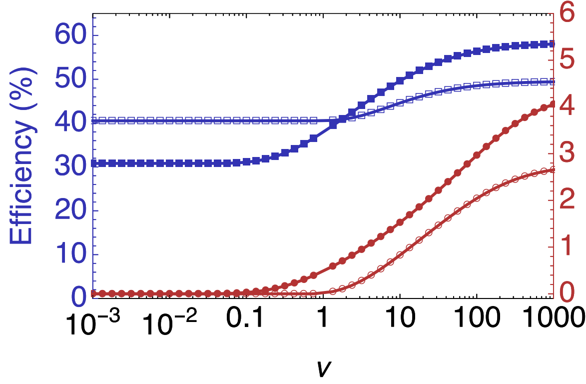

Fig. 2. Optimal efficiency (blue, squares) and thickness (red, circles) versus figure of merit $\nu_{\rm diff}$ for two IBSC's: Filled symbols show the optimal IBSC bandgaps, $E_g = 1.9$ eV, $E_{\rm CI} = 0.7$ eV, while empty symbols show a model of silicon with $E_g = 1.1$ eV, $E_{\rm CI} = 0.35$ eV. Both have fully concentrated blackbody sunlight and ideal n- and p-type regions. For small ν, the best IBSC has no IB region at all (i.e., the optical depth, OD, is small). For $\nu > 1$, significant improvements in efficiency are possible.

III. Predicting ν: A Case Study for a Dopant-Induced Intermediate Band in Si

A. *Simple Model for ν as a Function of Doping Concentration*

In this section, we develop simple models for α, τ, and μ in a dopant-produced IB system, combine them to predict optimal values of ν, and conclude with a discussion of how to estimate the current-matched IB filling fraction f. We use a simple neutral-impurity scattering model to make an upper estimate for μ. We relate α and τ to the subgap optical and electrical cross sections and the impurity concentration $N_{\rm I}$. Since α and τ for both electrons and holes are strongly affected by the filling fraction of the impurities f, the figures of merit for electrons and holes are strongly influenced by f. The key assumptions used in our model are as follows.

1) Both α_e and α_h are step functions, constant at all energies over their thresholds.
2) $\tau_{\rm e,h}$ follow the standard Shockley–Read form [10].
3) The number of IB states is equal to the impurity concentration $N_{\rm I}$.
4) To optimize IBSC performance, f is chosen such that the subgap generation rates are current matched.

For impurities with concentration $N_{\rm I}$ sufficiently low that each impurity site is effectively independent, the IB to CB optical transition has an absorptivity

$$\alpha_e = f N_{\rm I} \sigma_{\rm O}^e \tag{5}$$

where $\sigma_{\rm O}^e$ is the subgap optical cross section for the IB to CB process. Similarly, for the VB to IB transition, creating a hole, we have

$$\alpha_h = (1-f) N_{\rm I} \sigma_{\rm O}^h. \tag{6}$$

Generally, $\sigma_{\rm O}^e$ and $\sigma_{\rm O}^h$ are a function of photon energy. For the purposes of the simple model developed here, we approximate the optical cross sections as step functions, independent of photon energy above the relevant transition threshold. This approximation contrasts with the oft-made assumption of nonoverlapping absorptions [1], [19], [20] but is perhaps more accurate, especially when considering defects in the middle of the bandgap. When quoting literature results, we report peak values for subbandgap light. Note that large f increases electron generation and suppresses hole generation.

For highly doped IB materials, we expect that the dominant trapping and recombination processes for electrons and holes is through the IB states, which are deep in the gap [10]. The electron and hole trapping cross sections are $\sigma_{\rm T}^e$ and $\sigma_{\rm T}^h$ for the empty and filled dopant, respectively. The trapping times of electrons and holes are then

$$\tau_{\rm e} = \frac{1}{(1-f) N_{\rm I} \sigma_{\rm T}^e v_{\rm th}^e} \tag{7}$$

$$\tau_{\rm h} = \frac{1}{f N_{\rm I} \sigma_{\rm T}^h v_{\rm th}^h} \tag{8}$$

where $v_{\rm th}^e$ and $v_{\rm th}^h$ are thermal velocities of electrons and holes, respectively [10]. Note that large f increases electron lifetime and decreases hole lifetime.

The figure of merit ν depends on $\alpha^2 \tau \propto N_{\rm I}$; therefore, there is reason to believe that high dopant concentration will make effective devices. These high concentrations are beneficial because the IB region can be made thinner as $N_{\rm I}$ increases. There has been significant effort to achieve "lifetime recovery," an increase in τ with increasing $N_{\rm I}$, as predicted in [21]; recent arguments have questioned the existence of the effect [11], [13], and we do not consider it here. Lifetime recovery would make high $N_{\rm I}$ even more attractive.

When $N_{\rm I}$ is sufficiently small that impurity scattering is less important than intrinsic phonon scattering, μ is independent of $N_{\rm I}$. We estimate the dependence of μ on $N_{\rm I}$ by considering neutral impurity scattering $\mu_{\rm ni}$ [22], [23] and silicon's intrinsic phonon-scattering mobility $\mu_{\rm i}$ combined with Matthiessen's rule,

$$\mu^{-1} = \mu_{\rm ni}^{-1} + \mu_{\rm i}^{-1} \tag{9}$$

where

$$\mu_{\rm ni}^{e,h} = \frac{2\pi^3 q^3 m_{\rm e,h}^*}{5 N_{\rm I} \epsilon h^3} \tag{10}$$

where m^* is the carrier effective mass, q is the fundamental charge, h is Planck's constant, and ϵ is the static dielectric constant of the material. For example, using (2)–(10) with parameters for Si:S at $f = 1/2$, $\nu_{\rm e,drift}$ is shown in Fig. 3. It is clear that $\nu_{\rm e,drift}$ increases with $N_{\rm I}$ until μ becomes limited by the dopants and ν saturates at a value $\nu_{\rm e,drift}^*$. We can, thus, find an estimate of the maximum value of ν by considering dopants at the concentration where they become the limiting factor for the mobility. This observation also gives a simple estimate for the optimal dopant concentration for IB materials: $N_{\rm I}$ should be just at the level where the dopants limit the mobility.

Combining (2)–(10), the optimal ν is

$$\nu_e^* = \kappa_{\rm e} \frac{f^2}{1-f} \frac{(\sigma_{\rm O}^e)^2}{\sigma_{\rm T}^e} \tag{11}$$

$$\nu_h^* = \kappa_{\rm h} \frac{(1-f)^2}{f} \frac{(\sigma_{\rm O}^h)^2}{\sigma_{\rm T}^h} \tag{12}$$

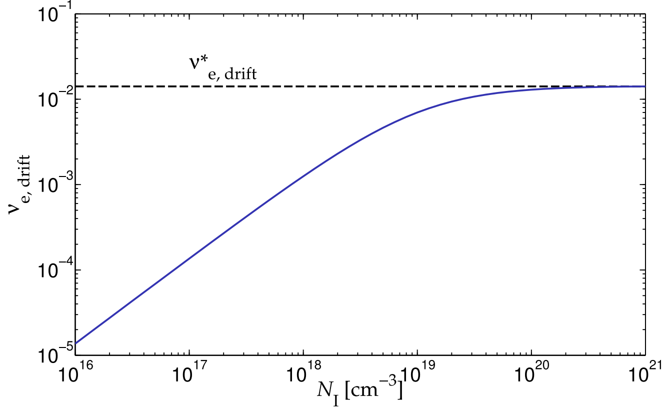

Fig. 3. Dependence of $\nu_{\mathrm{e,drift}}$ on dopant concentration for Si:S with $f = 1/2$ using (2)–(10) and parameters in Table II. The figure of merit $\nu_{\mathrm{e,drift}}$ increases linearly with N_{I} until the mobility becomes impurity limited, saturating at $\nu^*_{\mathrm{e,drift}}$.

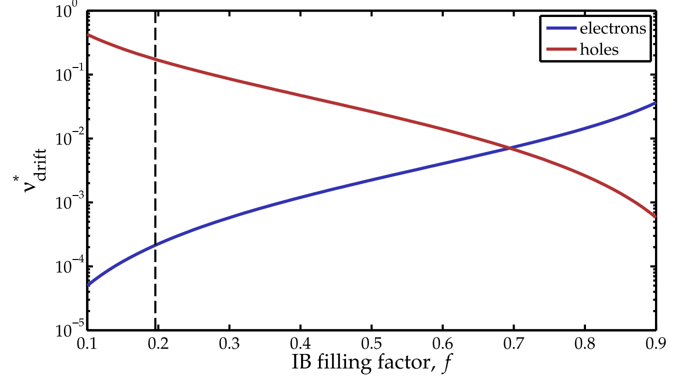

Fig. 4. Maximal figures of merit from (11) and (12) as a function of impurity filling fraction f for the case of Si:Fe with parameters from Tables I and II. The figures of merit vary considerably with f. Under the approximation of a frequency-independent optical cross section (above the energy-conservation threshold), the current-matching f given by (17) is indicated by the vertical dashed line. In this example, at least one of ν^e_{drift}, ν^h_{drift} is small for all values of f, indicating a material system without good prospects for IBSC.

where κ_{e}, κ_{h} are constants dependent on properties of the host semiconductor and whether the system is in the drift or diffusion limit. We see that the ideal IB-forming dopant has large subgap optical cross sections σ_{O} and small trapping cross sections, σ_{T}. For the drift-limited case,

$$\kappa_{\mathrm{e}} = \frac{2E_{\mathrm{g}}\pi q^2 m^*_{\mathrm{e}}}{5\epsilon h^3 v^e_{\mathrm{th}}} \tag{13}$$

$$\kappa_{\mathrm{h}} = \frac{2E_{\mathrm{g}}\pi q^2 m^*_{\mathrm{h}}}{5\epsilon h^3 v^h_{\mathrm{th}}}. \tag{14}$$

For the diffusion-limited case, E_g is replaced by $k_{\mathrm{b}}T$.

Note that ν_e and ν_h are highly dependent on f. Although the equilibrium filling factor can be controlled by codoping, one cannot simply choose f to maximize the smaller of ν_e and ν_h. For an effective IBSC, f must be chosen to ensure current matching between the two subgap optical transitions [24], [25]. If the filling factor is maintained unequal to the current-matched f, then the excess flow of only one carrier type will result in charge transfer out of the IB, resulting in deleterious internal voltage drops. If the current-matching f is not the equilibrium value, then it may be achieved by photofilling if the IB density of states is sufficiently small [26], [27]. If the current-matched f cannot be achieved by photofilling, then codoping to set f at the current-matching condition is desirable. In evaluating the figures of merit, f should not be considered to be a design parameter. Rather, based on the energetic position of the IB and the values of $\sigma^{e,h}_{\mathrm{O}}$, we should estimate the current-matched value of f and use it to evaluate ν. The large effect that f can have on ν is indicated in Fig. 4.

The simplest estimate of ν is made by taking $f = 1/2$, which is also the optimal value if $\sigma^e_{\mathrm{O}} = \sigma^h_{\mathrm{O}}$, and there is an equal flux of photons that can be absorbed by each transition (e.g., the IB is at the current-matched energy with nonoverlapping absorptions [1]). When these conditions do not hold, f can in general be nonuniform [28]. The full prediction of a photofilled f at steady state requires ensuring that, at each location, the sum of generation, recombination, and carrier transport is zero [27]. Such a calculation can be performed for any material of interest, but our goal here is to make a simple model that captures the key physics, for the purposes of early screening. Promising systems are then worth detailed modeling. Thus, we approximate f as uniform in our IB material, which can be achieved with sufficiently large carrier mobility in the IB or can be considered as the average f in a more sophisticated model. The photogeneration rates from VB to IB and IB to CB are, respectively,

$$G_h = F_h\alpha_h \tag{15}$$

$$G_e = F_e\alpha_e \tag{16}$$

where F_e is the flux of subgap photons with energy between E_{CI} and E_g, and F_h is the flux of subgap photons with energy between E_{IV} and E_g, with energies indicated in Fig. 1. In the interest of simplicity, we estimate the current-matched f by setting $G_h = G_e$, which requires photogeneration to be equal and neglects the effects of recombination processes entirely. From a device-modeling perspective, this is a crude approximation, but it captures the qualitative features of a more complicated photofilling model [27]. Using (5) and (6),

$$f_{\mathrm{cm}} = \frac{F_h\sigma^h_{\mathrm{O}}}{F_h\sigma^h_{\mathrm{O}} + F_e\sigma^e_{\mathrm{O}}}. \tag{17}$$

Literature values for both electron and hole optical cross sections were not found for all elements. For elements with only one set of cross sections, we use $f = 1/2$; note that if the current-matched f deviates significantly from $1/2$, figures of merit in an actual device could be significantly different.

B. Results for Dopants in Si

With these results, we can use literature values for the optical and electrical trapping cross sections for impurities in silicon to estimate ν for IB materials. The literature values are shown in Tables I and II. In some cases, data exist for only one of the carrier types (e.g., σ^e_{T} or σ^h_{T}). Fig. 5 shows the resulting estimates of the optimal ν_{drift} for a number of dopants in silicon. We consider the optimistic drift case where the IB is assumed

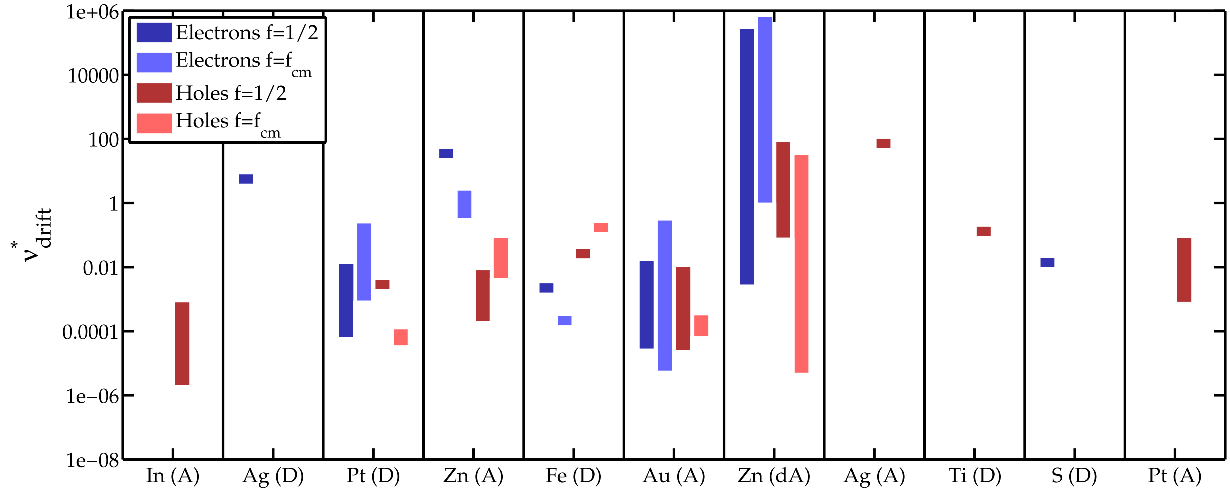

Fig. 5. Estimate of the maximum value of the figure of merit $\nu_{\rm drift}$ for electrons and holes for a variety of deep-level dopants in silicon, based on the model of Section III and literature values for cross sections reported in Tables I and II. When data exist for both electron and hole cross sections of the defect, we find the simple current-matching f using (17) and produce the current-matched estimates for the optimal $\nu_{\rm drift}$. For cases where there is a range of cross sections in the literature, the solid band indicates the range of possible values of ν. Acceptors are marked by "A," donors by "D," and "dA" indicates double acceptor. Elements are in order of defect energy from VB to CB; see Tables I and II.

TABLE I
ELECTRICAL AND OPTICAL CROSS SECTIONS FOR HOLES FOR DOPANTS IN SILICON

Dopant	Energy [meV]	$\sigma_{\rm T}^h$ [cm^2]	$\sigma_{\rm O}^h$ [cm^2]	Source
In (A)	$E_{\rm V}+157$	1×10^{-13}	4.5×10^{-17} to 2×10^{-16}	[33], [34]
Pt (D)	$E_{\rm V}+260$ to $E_{\rm V}+320$	1×10^{-16}	5×10^{-15} to 1×10^{-14}	[35], [34]
Zn (A)	$E_{\rm V}+310$	10^{-14} to 10^{-13}	2×10^{-16}	[36]
Fe$_{\rm i}$ (D)	$E_{\rm V}+380$	7×10^{-17}	3×10^{-17}	[37], [38]
Au (A)	$E_{\rm V}+560$ to $E_{\rm V}+630$	8×10^{-15}	1×10^{-17} to 2×10^{-16}	[34]
Zn (dA)	$E_{\rm V}+580$	10^{-16} to 10^{-13}	2×10^{-15}	[36]
Ag (A)	$E_{\rm C}-290$	7×10^{-16}	5×10^{-15}	[39], [40]
Ti (D)	$E_{\rm C}-270$ to $E_{\rm C}-260$	1.4×10^{-15}	3×10^{-16}	[39], [37]
Pt (A)	$E_{\rm C}-230$ to $E_{\rm C}-200$	1×10^{-17} to 6×10^{-15}	2×10^{-17}	[39], [34]

Optical cross sections are the maximum reported values.

TABLE II
ELECTRICAL AND OPTICAL CROSS SECTIONS FOR ELECTRONS FOR DOPANTS IN SILICON

Dopant	Energy [meV]	$\sigma_{\rm T}^e$ [cm^2]	$\sigma_{\rm O}^e$ [cm^2]	Source
In (A)	$E_{\rm V}+157$	2×10^{-22}	-	[41]
Ag (D)	$E_{\rm V}+260$	2×10^{-15}	2×10^{-15}	[39], [40]
Pt (D)	$E_{\rm V}+260$ to $E_{\rm V}+320$	3×10^{-17}	2×10^{-16} to 4×10^{-14}	[34], [35]
Zn (A)	$E_{\rm V}+310$	5×10^{-16} to 10^{-15}	3×10^{-15}	[36]
Fe$_{\rm i}$ (D)	$E_{\rm V}+380$	5×10^{-14}	2×10^{-16}	[37], [38]
Au (A)	$E_{\rm V}+560$ to $E_{\rm V}+630$	7×10^{-17} to 4×10^{-15}	2×10^{-17}	[39], [37], [34]
Zn (dA)	$E_{\rm V}+580$	10^{-20} to 10^{-16}	10^{-17} to 10^{-15}	[36]
S (D)	$E_{\rm C}-250$	2×10^{-15}	2×10^{-16}	[42], [43]

Optical cross sections are the maximum reported values.

to be in the depletion region, as it presents the upper limit for ν. Achieving these values of ν generally requires large dopant concentrations. Sullivan *et al.* [12] demonstrated that, for the Si:S system, the properties of the material at high dopant concentration can be well approximated using the cross sections from the dilute impurity limit. For Au, Pt, and Ti, there is uncertainty about the energetic position of the defect state, which is reflected in the tables and in the calculations of $f_{\rm cm}$ in Fig. 5.

For all dopants, Fig. 5 shows the figures of merit in the case of half-filling, $f = 1/2$. For dopants with data on optical cross sections for both subgap transitions, we use (17) to estimate the current-matched f. We then present $\nu^*_{\rm drift}$ with $f = f_{\rm cm}$. In the case of Zn and Fe, this change is significant. It would be desirable to turn the results of Fig. 5 into predicted device efficiencies, for example using the model of Fig. 2. Since any device model requires many material and device properties, including how much overlap to consider in the absorptivities corresponding to the three transitions, we do not find a generic and simple way to convert Fig. 5 into predicted efficiencies. Rather, since large ν is a necessary condition for high efficiency IBSC, those cases with potential indicated by Fig. 5 are worthy of further study, including detailed modeling.

Since both ν_e and ν_h must be large for high efficiency, these results predict, in advance of material growth, that elements such as platinum (donor), gold (acceptor), and iron (donor) will not produce an effective IBSC even with enhancements from light trapping. The zinc single acceptor only holds promise if sufficient light trapping can be implemented. We do not have enough information on both transitions for dopants such as sulfur, titanium, indium, and platinum (acceptor), but these can be effective only with significant light trapping or if the current-matched f is significantly less than 1/2 (for titanium, indium, and platinum acceptor) or significantly greater than 1/2 (for sulfur). Although we do not have data for both carrier types, silver (as either donor or acceptor) presents a good possibility,

as does the zinc double acceptor, which could be accessed using codoping with a shallow donor such as phosphorus [29]. Si:Au has recently been shown to produce measurable subgap photocurrent, but with a quantum efficiency less than 10^{-4} [30], consistent with the low predicted values for ν in Fig. 5. Si:Ti has been extensively studied for IBSC [31], [32]. There are, additionally, a large number of dopants to study that do not appear in Fig. 5. Since research has likely been biased toward studying the properties of dopants with the worst effects on lifetime, we speculate that other elements may have better properties for IBSC.

IV. Conclusion

We have described the figure of merit ν for IBSC's and detailed a simple model for the dependence of its constituent parameters (μ, α, and τ) on the optical and electrical cross sections, doping concentration, and filling factor in a dopant-produced IB. To achieve high efficiency, both the electron and hole figures of merit, ν_e and ν_h, must be large. High efficiency has additional requirements, such as bandgaps well matched the solar spectrum and a filling factor f permitting current matching of the subgap transitions. In the spirit of a simple model for screening purposes, we introduce an approximation to the current-matched f for the dopant-produced IB, which then allows a prediction for the optimal ν that can be achieved in the material.

We report ranges of possible figures of merit for several dopants in silicon, highlighting particularly appealing dopants for further study (silver and the zinc double acceptor). This procedure for estimating the optimal figure of merit for a system, illustrated for dopants in silicon, can be used for dopant-formed IB materials in other semiconductors. It can also be readily adapted to quantum-dot or alloy-based IB materials, as long as a theory of the effect of quantum dot or alloy concentration on absorption, mobility, and lifetime is developed. The figure of merit ν presents a simple organizing principle for the targeted search for IB materials and further enables an easy estimate of the ideal concentration of dopants or quantum dots in the material, in advance of detailed modeling of a particular material system.

Acknowledgent

The authors would like to acknowledge helpful discussions with M. T. Winkler.

References

[1] A. Luque and A. Martí, "Increasing the efficiency of ideal solar cells by photon induced transitions at intermediate levels," *Phys. Rev. Lett.*, vol. 78, no. 26, pp. 5014–5017, 1997.

[2] W. Shockley and H. J. Queisser, "Detailed balance limit of efficiency of p-n junction solar cells," *J. Appl. Phys.*, vol. 32, no. 3, pp. 510–519, 1961.

[3] A. Luque, A. Martí, and C. Stanley, "Understanding intermediate-band solar cells," *Nat. Photon*, vol. 6, no. 3, pp. 146–152, 2012.

[4] T. Tanaka, K. M. Yu, A. X. Levander, O. D. Dubon, L. A. Reichertz, N. Lopez, M. Nishio, and W. Walukiewicz, "Demonstration of $ZnTe_{1-x}O_x$ intermediate band solar cell," *Jpn. J. Appl. Phys.*, vol. 50, no. 8R, p. 082304, 2011.

[5] N. Ahsan, N. Miyashita, M. M. Islam, K. M. Yu, W. Walukiewicz, and Y. Okada, "Two-photon excitation in an intermediate band solar cell structure," *Appl. Phys. Lett.*, vol. 100, no. 17, pp. 172111-1–172111-4, 2012.

[6] T. Tanaka, M. Miyabara, Y. Nagao, K. Saito, Q. Guo, M. Nishio, K. M. Yu, and W. Walukiewicz, "Photocurrent induced by two-photon excitation in ZnTeO intermediate band solar cells," *Appl. Phys. Lett.*, vol. 102, no. 5, pp. 052111-1–052111-4, 2013.

[7] T. Sogabe, Y. Shoji, M. Ohba, K. Yoshida, R. Tamaki, H.-F. Hong, C.-H. Wu, C.-T. Kuo, S. TomiÄ, and Y. Okada, "Intermediate-band dynamics of quantum dots solar cell in concentrator photovoltaic modules," *Sci. Rep.*, vol. 4, p. 4792, 2014.

[8] W. Wang, A. S. Lin, and J. D. Phillips, "Intermediate-band photovoltaic solar cell based on ZnTe:O," *Appl. Phys. Lett.*, vol. 95, no. 1, pp. 011103-1–011103-3, 2009.

[9] N. López, L. A. Reichertz, K. M. Yu, K. Campman, and W. Walukiewicz, "Engineering the electronic band structure for multiband solar cells," *Phys. Rev. Lett.*, vol. 106, no. 2, p. 028701, 2011.

[10] W. Shockley and W. T. Read, "Statistics of the recombinations of holes and electrons," *Phys. Rev.*, vol. 87, no. 5, pp. 835–842, 1952.

[11] J. J. Krich, B. I. Halperin, and A. Aspuru-Guzik, "Nonradiative lifetimes in intermediate band photovoltaics—absence of lifetime recovery," *J. Appl. Phys.*, vol. 112, no. 1, pp. 013707–013708, 2012.

[12] J. T. Sullivan, C. B. Simmons, J. J. Krich, A. J. Akey, D. Recht, M. J. Aziz, and T. Buonassisi, "Methodology for vetting heavily doped semiconductors for intermediate band photovoltaics: A case study in sulfur-hyperdoped silicon," *J. Appl. Phys.*, vol. 114, no. 10, pp. 103701-1–103701-9, 2013.

[13] M.-J. Sher, C. B. Simmons, J. J. Krich, A. J. Akey, M. T. Winkler, D. Recht, T. Buonassisi, M. J. Aziz, and A. M. Lindenberg, "Picosecond carrier recombination dynamics in chalcogen-hyperdoped silicon," *Appl. Phys. Lett.*, vol. 105, no. 5, p. 053905, 2014.

[14] R. Strandberg, "Evaluation of a selection of intermediate band materials based on their absorption coefficients," *IEEE J. Photovoltaics*, vol. 3, no. 3, pp. 997–1003, Jul. 2013.

[15] J. J. Krich, A. H. Trojnar, L. Feng, K. Hinzer, and A. W. Walker, "Modeling intermediate band solar cells: A roadmap to high efficiency," in *Proc. SPIE*, vol. 8981, pp. 898100-1–898100-8, 2014.

[16] E. Yablonovitch, "Statistical ray optics," *J. Opt. Soc. Amer.*, vol. 72, no. 7, pp. 899–907, 1982.

[17] O. D. Miller, E. Yablonovitch, and S. R. Kurtz, "Strong internal and external luminescence as solar cells approach the Shockley-Queisser limit," *IEEE J. Photovoltaics*, vol. 2, no. 3, pp. 303–311, Jul. 2012.

[18] J. Nelson, *The Physics of Solar Cells*. London, U.K.: Imperial College Press, 2003.

[19] L. Cuadra, A. Martí, and A. Luque, "Influence of the overlap between the absorption coefficients on the efficiency of the intermediate band solar cell," *IEEE Trans. Electron Devices*, vol. 51, no. 6, pp. 1002–1007, Jun. 2004.

[20] E. López, A. Martí, E. Antolín, and A. Luque, "Limiting efficiency of silicon intermediate band solar cells," in *Proc. Photovoltaic Spec. Conf.*, 2014.

[21] A. Luque, A. Martí, E. Antolín, and C. Tablero, "Intermediate bands versus levels in non-radiative recombination," *Physica B*, vol. 382, nos. 1/2, pp. 320–327, 2006.

[22] S. S. Li and W. Thurber, "The dopant density and temperature dependence of electron mobility and resistivity in n-type silicon," *Solid-State Electron.*, vol. 20, no. 7, pp. 609–616, 1977.

[23] C. Erginsoy, "Neutral impurity scattering in semiconductors," *Phys. Rev.*, vol. 79, no. 6, pp. 1013–1014, 1950.

[24] A. S. Brown and M. A. Green, "Impurity photovoltaic effect: Fundamental energy conversion efficiency limits," *J. Appl. Phys.*, vol. 92, no. 3, pp. 1329–1336, 2002.

[25] A. Martí, E. Antolín, P. García-Linares, I. Ramiro, I. Artacho, E. López, E. Hernández, M. J. Mendes, A. Mellor, I. Tobías, D. Fuertes Marrón, C. Tablero, A. B. Cristóbal, C. G. Bailey, M. Gonzalez, M. Yakes, M. P. Lumb, R. Walters, and A. Luque, "Six not so easy pieces in intermediate band solar cell research," *J. Photon. Energy*, vol. 3, pp. 86200J-1–86200J-11, 2013.

[26] R. Strandberg and T. W. Reenaas, "Photofilling of intermediate bands," *J. Appl. Phys.*, vol. 105, no. 12, pp. 124512–124518, 2009.

[27] R. Strandberg and T. W. Reenaas, "Drift-diffusion model for intermediate band solar cells including photofilling effects," *Prog. Photovoltaic, Res. Appl.*, vol. 19, no. 1, pp. 21–32, 2011.

[28] R. Strandberg and T. W. Reenaas, "Optimal filling of the intermediate band in idealized intermediate-band solar cells," *IEEE Trans. Electron Devices*, vol. 58, no. 8, pp. 2559–2565, Aug. 2011.

[29] C. B. Simmons, A. J. Akey, J. P. Mailoa, D. Recht, M. J. Aziz, and T. Buonassisi, "Enhancing the infrared photoresponse of silicon by controlling the fermi level location within an impurity band," *Adv. Funct. Mater.*, vol. 24, no. 19, pp. 2852–2858, 2014.

[30] J. P. Mailoa, A. J. Akey, C. B. Simmons, D. Hutchinson, J. Mathews, J. T. Sullivan, D. Recht, M. T. Winkler, J. S. Williams, J. M. Warrender, P. D. Persans, M. J. Aziz, and T. Buonassisi, "Room-temperature subband gap optoelectronic response of hyperdoped silicon," *Nat. Commun.*, vol. 5, p. 3011, 2014.

[31] J. Olea, M. Toledano-Luque, D. Pastor, G. González-Díaz, and I. Mártil, "Titanium doped silicon layers with very high concentration," *J. Appl. Phys.*, vol. 104, no. 1, pp. 016105-1–016105-3, 2008.

[32] D. Pastor, J. Olea, A. del Prado, E. García-Hemme, R. García-Hernansanz, and G. González-Díaz, "Insulator to metallic transition due to intermediate band formation in Ti-implanted silicon," *Sol. Energy Mater. Sol. Cells*, vol. 104, pp. 159–164, 2012.

[33] W. Schelter, W. Hell, R. Helbig, and M. Schulz, "Optical properties of indium-doped silicon reinspected," *J. Phys. C*, vol. 15, pp. 5839–5850, 2013.

[34] J. Chen and A. Milnes, "Energy-levels in silicon," *Annu. Rev. Mater. Sci.*, vol. 10, pp. 157–228, 1980.

[35] S. Braun, H. Grimmeiss, and K. Spann, "Photoionization cross sections in platinum-doped silicon," *J. Appl. Phys.*, vol. 48, pp. 3883–3887, 1977.

[36] A. Sklensky, and R. Bube, "Photoelectronic properties of zinc impurity in silicon," *Phys. Rev. B*, vol. 6, pp. 1328–1336, 1972.

[37] D. Macdonald and L. Geerligs, "Recombination activity of interstitial iron and other transition metal point defects in p- and n-type crystalline silicon," *Appl. Phys. Lett.*, vol. 85, pp. 4061–4063, 2004.

[38] K. Wünstel, K. Froehner, and P. Wagner, "Iron-related defects in silicon," *Physica B*, vol. 116, pp. 301–305, 1983.

[39] M. Okuyama, N. Matsunaga, J. Chen, and A. Milnes, "Photoionization cross-section and energy levels of gold, iron, platinum, silver, and titanium," *J. Electron. Mater.*, vol. 8, pp. 501–515, 1979.

[40] F. Thiel, "Electronic properties of silicon doped with silver," *J. Appl. Phys.*, vol. 41, pp. 254–263, 1970.

[41] B. Sundström, L. Huldt, and N. Nilsson, "Electron capture coefficient of neutral indium and pair recombination in compensated silicon," *J. Phys. C*, vol. 15, pp. 3359–3370, 1982.

[42] T. Ning, and C. Sah, "Photoionization cross sections of a two-electron donor center in silicon," *Phys. Rev. B*, vol. 14, pp. 2528–2533, 1976.

[43] H. Grimmeiss, E. Janzén, and B. Skarstam, "Deep sulfur-related centers in silicon," *J. Appl. Phys.*, vol. 51, pp. 4212–4217, 1980.

Authors' photographs and biographies not available at the time of publication.